

This is a postprint version of the following published document:

Martínez-Ruiz, D., Huete, C., Sánchez, A. L., &
Williams, F. A. (2020). Theory of Weakly Exothermic
Oblique Detonations. *AIAA Journal*, 58(1), 236–242.

DOI: <https://doi.org/10.2514/1.j058460>

© 2019 by the American Institute of Aeronautics
and Astronautics, Inc. All rights reserved.

Theory of Weakly Exothermic Oblique Detonations

Daniel Martínez-Ruiz *

ETSIAE, Universidad Politécnica de Madrid, Madrid, 28040, Spain

César Huete[†]

Universidad Carlos III de Madrid, Spain.

Antonio L. Sánchez[‡] and Forman A. Williams[§]

University of California San Diego, La Jolla, CA 92093-041

A simplified formulation, based on treating the ratio of the heat release to the post-shock thermal enthalpy as a small parameter, accommodating arbitrary chemistry descriptions, is shown to reproduce computationally the same variety of phenomena as more complex formulations for oblique detonations with supersonic post-shock flow. The resulting small relative variations of velocity and thermodynamic properties across the reaction region are described by linearized Euler equations written in characteristic form, supplemented by the linearized Rankine-Hugoniot jump conditions across the leading shock. Analysis of the interaction of the oblique detonation with a weak vortex sheet, for an Arrhenius irreversible reaction with an activation energy large compared with the post-shock thermal enthalpy, reveals that, as β , the product of the activation energy and the heat release divided by the square of the post-shock thermal enthalpy, increases through values of order unity, decaying spatial oscillations, found for small values, are replaced by persistent nonlinear oscillations of finite amplitude for larger values. Beyond a critical value of β the growth of the oscillation amplitude leads to the development of a singularity at the shock, an explosion, consistent with the formation of a triple point. Many related problems can be clarified with this formulation.

Nomenclature

A_T, A_p, A_v	=	Rankine-Hugoniot factors, defined in Eq. (A.13)
B_T, B_p, B_v	=	Rankine-Hugoniot factors, defined in Eq. (A.13)
$F_\rho, F_p, F_T, F_M, F_v$	=	Rankine-Hugoniot functions, defined in Eqs. (A.6)–(A.10)
p	=	pressure
q	=	dimensionless heat of reaction

*Lecturer, Universidad Politécnica de Madrid, Spain.

[†]Associate Professor, Fluid Mechanics Group, Universidad Carlos III de Madrid, Spain.

[‡]Professor, Department of Mechanical and Aerospace Engineering, University of California San Diego.

[§]Professor, Department of Mechanical and Aerospace Engineering, University of California San Diego. AIAA Fellow.

Q	=	heat released per unit mass of reactant mixture
Q'	=	heat released per unit mass of fuel
T	=	temperature
U	=	streamwise velocity
V	=	transverse velocity
y	=	normalized reactant mass fraction
Y_i	=	mass fraction of species i
β	=	dimensionless activation energy, defined in Eq. (28)
ν	=	counterclockwise flow deflection
Ω	=	dimensionless heat-release rate
ϕ_o	=	inclination of the post-shock flow with respect to the shock
ρ	=	density
σ	=	incident angle

Subscripts

u	=	properties upstream from the front
o	=	properties at the Neumann spike
b	=	equilibrium burnt-gas properties

Accents

bar	=	base-flow properties
hat	=	dimensionless perturbed properties

I. Introduction

OBLIQUE detonations are ubiquitous in supersonic propulsion applications, including Ram Accelerators and Oblique-Detonation-Wave Engines [1]. The strongly nonlinear character of the flow hinders associated experimental and computational investigations. As a result, despite significant computational discoveries, beginning with the work of Li, Kailasanath and Oran [2–8], many aspects of the formation, dynamics, and stability of oblique detonations remain unclear. Computational findings include the existence of smooth and abrupt transitions within oblique detonations [4, 5, 7] and the development of cellular-like spatial oscillations along oblique detonation fronts [6, 8]. A complete parametric specification of the conditions under which the different structures of oblique detonations may occur is, however, still lacking.

Simplified models can be instrumental in developing an understanding of the complicated physicochemical interactions that determine detonation stability and response to disturbances. For instance, simplifications arising in

hypersonic systems have been exploited in perturbation analyses using the reciprocal of the square of the incident Mach number as an asymptotically small parameter [9]. The present paper focuses instead on simplifications arising when the heat released by the chemical reaction is small compared with the post-shock thermal enthalpy, a situation favored by strong leading shock waves or sufficiently fuel-lean reactant mixtures. Under these weakly exothermic conditions the relative changes of the different flow variables, of order unity across the leading shock, remain small across the reaction region. Correspondingly, most of the terms in the conservation equations for the post-shock flow can be linearized about the unperturbed post-shock state. The predominant exception to this useful linearization appears in the chemistry terms in systems effectively involving large-activation-energy reactions, whose nonlinear character for many purposes often can be described with use made of the Frank-Kamenetskii approximation for the exponential temperature dependence, a linearization within the exponential. Similar linearizations have been found to be useful for addressing diffusion-flame ignition by impingement of a shock wave on a mixing layer [10, 11]. Other simplifications through the invocation of asymptotic limits, such as the Newtonian limit of near-unity specific-heat ratios, often used in analytical work pertaining to detonation dynamics [12], are not useful for the present problem because it turns out to be important that the small relative changes of pressure and temperature remain comparable in magnitude, rather than temperature changes being smaller.

The formulation of the problem for fully supersonic flow with small heat release is given in the next section, with the shock jump conditions and their linearization given in the appendix. The simplification of the heat-release rate and the application to a detonation with a vortex sheet separating two supersonic parallel streams having slightly different Mach numbers is then presented in following sections. Finally, conclusions and worthwhile future work will be summarized.

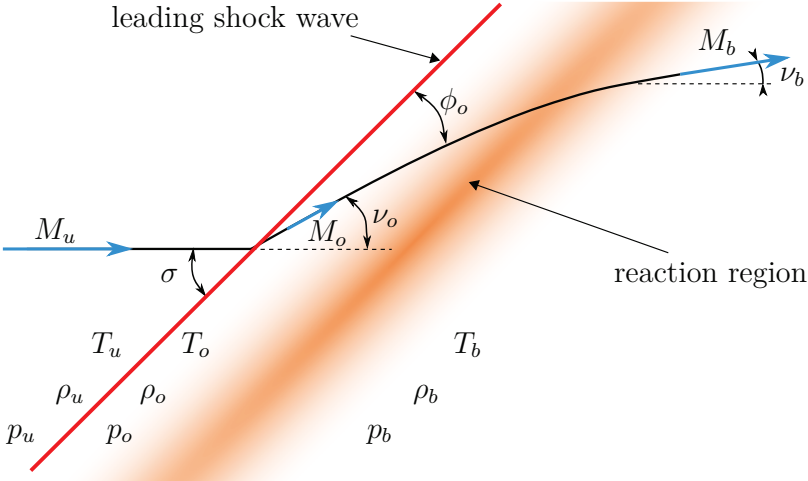


Fig. 1 Illustration of the structure of the oblique detonation.

II. Formulation

The well-known ZND structure of oblique detonations, schematically represented in Fig. 1, involves a leading shock wave followed by a reaction region. In the notation employed, flow properties upstream from the shock are denoted by the subscript u , whereas the subscript o is used for the gas state immediately downstream from the shock and the subscript b identifies the final equilibrium burnt-gas properties. For an oblique detonation with incident angle σ and incident Mach number M_u , the changes in density ρ , pressure p , temperature T , and Mach number M from the upstream values as well as the counterclockwise flow deflection ν can be computed with use made of the Rankine-Hugoniot equations [13]. The jump conditions across the oblique detonation [14] appear in the appendix, where their linearization appropriate for the present formulation is presented.

The mathematical problem describing the structure and dynamics of oblique detonations can be simplified for configurations with small heat release $Q \ll c_p T_o$. Equations will be written for the small flow departures from a predetermined base flow, defined by the constant incident angle $\bar{\sigma}$ and the upstream values of the Mach number \bar{M}_u , pressure \bar{p}_u , temperature \bar{T}_u , and density $\bar{\rho}_u$. Corresponding post-shock properties for this base solution are given by

$$\frac{\bar{T}_o}{\bar{T}_u} = F_T(\bar{M}_u, \bar{\sigma}), \quad \frac{\bar{p}_o}{\bar{p}_u} = F_p(\bar{M}_u, \bar{\sigma}), \quad \frac{\bar{\rho}_o}{\bar{\rho}_u} = F_\rho(\bar{M}_u, \bar{\sigma}), \quad \bar{M}_o = F_M(\bar{M}_u, \bar{\sigma}), \quad \bar{\nu}_o = F_\nu(\bar{M}_u, \bar{\sigma}) \quad (1)$$

in terms of the Rankine-Hugoniot expressions given by Eqs. (A.6)–(A.10) of the appendix. The value of the post-shock velocity can be evaluated in terms of \bar{M}_o and \bar{T}_o with use made of

$$\bar{U}_o = \bar{M}_o \sqrt{(\gamma - 1)c_p \bar{T}_o}. \quad (2)$$

As seen in Eq. (A.12) of the appendix, the relative changes in flow properties resulting from the chemical heat release behind the shock are of order

$$q = \frac{Q}{c_p \bar{T}_o} \ll 1. \quad (3)$$

Since the flow deflection across the reaction region is small, the streamlines are almost exactly aligned with the post-shock unperturbed flow, thereby motivating the introduction of the cartesian coordinate system (s, n) indicated in Fig. 2, with the streamwise coordinate s and the transverse coordinate n scaled with the induction length $\bar{U}_o t_i$ based on the characteristic induction time t_i at temperature \bar{T}_o , a quantity that depends on the underlying chemistry description. The origin of the reference frame lies at the leading shock, at a point to be selected to simplify the description of the problem at hand. The associated streamwise and transverse velocity components will be denoted by U and V , with the latter related to the flow deflection by $V/\bar{U}_o = \nu - \bar{\nu}_o$. In the limit defined in Eq. (3) the chemical reaction results in small relative variations of the different flow variables, which can be described with the linearized form of the governing

equations, including the continuity, momentum, and energy conservation equations

$$\frac{\partial \hat{\rho}}{\partial s} + \frac{\partial \hat{U}}{\partial s} + \frac{\partial \hat{V}}{\partial n} = 0 \quad (4)$$

$$\gamma \bar{M}_o^2 \frac{\partial \hat{U}}{\partial s} + \frac{\partial \hat{p}}{\partial s} = 0 \quad (5)$$

$$\gamma \bar{M}_o^2 \frac{\partial \hat{V}}{\partial s} + \frac{\partial \hat{p}}{\partial n} = 0 \quad (6)$$

$$\frac{\partial \hat{T}}{\partial s} - \frac{\gamma - 1}{\gamma} \frac{\partial \hat{p}}{\partial s} = \Omega, \quad (7)$$

written in terms of the dimensionless order-unity variables

$$\hat{\rho} = \frac{(\rho - \bar{\rho}_o)/\bar{\rho}_o}{q}, \hat{p} = \frac{(p - \bar{p}_o)/\bar{p}_o}{q}, \hat{T} = \frac{(T - \bar{T}_o)/\bar{T}_o}{q}, \hat{U} = \frac{(U - \bar{U}_o)/\bar{U}_o}{q}, \text{ and } \hat{V} = \frac{V/\bar{U}_o}{q}. \quad (8)$$

The above equations must be supplemented with the equation of state written in the linearized form

$$\bar{p} = \hat{\rho} + \hat{T}, \quad (9)$$

corresponding to constant mean molecular weight, an appropriate simplification for reactant mixtures satisfying the condition stated in Eq. (3). Besides, since the dimensionless heat-release rate Ω (the amount of heat released per unit volume per unit time scaled with $\bar{\rho}_o Q/t_i$) depends in general on the local composition, the solution requires simultaneous integration of an additional set of conservation equations describing the evolution of the relevant chemical species along the streamlines $n = \text{constant}$, given by

$$\frac{\partial Y_i}{\partial s} = -\omega_i/(\bar{\rho}_o/t_i), \quad (10)$$

where Y_i and $\omega_i(\hat{T}, Y_i)$ are the mass fraction and the mass consumption rate of chemical species i , respectively. Since the shock is chemically frozen, the accompanying boundary conditions at the shock reduce to $Y_i = Y_{i_u}$ in terms of the known upstream mass fractions Y_{i_u} in the incoming stream.

The problem can be simplified by eliminating \hat{U} and \hat{p} with use made of Eqs. (4), (5), and (9) to give

$$\frac{\gamma \bar{M}_o^2 - 1}{\gamma \bar{M}_o^2} \frac{\partial \hat{p}}{\partial s} - \frac{\partial \hat{T}}{\partial s} + \frac{\partial \hat{V}}{\partial n} = 0. \quad (11)$$

Equations (6), (7), and (11) constitute a convenient starting set of conservation equations for \hat{T} , \hat{p} , and \hat{V} . The change of the incident angle $\hat{\sigma} = (\sigma - \bar{\sigma})/q \sim 1$ is an additional variable of the problem, which enters through the boundary conditions for \hat{T} , \hat{p} , and \hat{V} at the leading shock. These can be determined by linearizing the Rankine-Hugoniot

Eqs. (A.7)–(A.10) in the appendix to give

$$\hat{T} = \hat{T}_u + A_T \hat{M}_u + B_T \hat{\sigma}, \quad \hat{p} = A_p \hat{M}_u + B_p \hat{\sigma}, \quad \hat{V} = A_v \hat{M}_u + B_v \hat{\sigma} \quad (12)$$

involving the coefficients

$$A_T = \frac{1}{F_T} \frac{\partial F_T}{\partial M_u}, B_T = \frac{1}{F_T} \frac{\partial F_T}{\partial \sigma}, A_p = \frac{1}{F_p} \frac{\partial F_p}{\partial M_u}, B_p = \frac{1}{F_p} \frac{\partial F_p}{\partial \sigma}, A_v = \frac{\partial F_v}{\partial M_u}, B_v = \frac{\partial F_v}{\partial \sigma}, \quad (13)$$

to be evaluated at $M_u = \bar{M}_u$ and $\sigma = \bar{\sigma}$ from the expressions given in Eq. (A.13). For generality, the jumps described by Eq. (12) account for the possible existence of small fluctuations of order q in the Mach number and temperature of the approaching stream, described by the known order-unity functions $\hat{T}_u = [(T_u - \bar{T}_u)/\bar{T}_u]/q$ and $\hat{M}_u = (M_u - \bar{M}_u)/q$. This generalization is needed, for example, in studies of occurrence of vortical and entropic burnt-gas oscillations in detonations subjected to non-uniformities of velocity and temperature of the approaching stream [15].

The solution simplifies when the post-shock flow is supersonic, i.e. $\bar{M}_o > 1$, as occurs when the values of the incident Mach number \bar{M}_u and incident angle $\bar{\sigma}$ place the system below the upper thick curve of the figure in the appendix. The Euler equations can be formulated in characteristic form, with three different characteristic curves crossing any given point, i.e. the streamline and the two Mach lines C_{\pm} , the latter crossing the streamline with local angles $\pm\mu$ with $\mu = \sin^{-1}(M^{-1})$ [16].

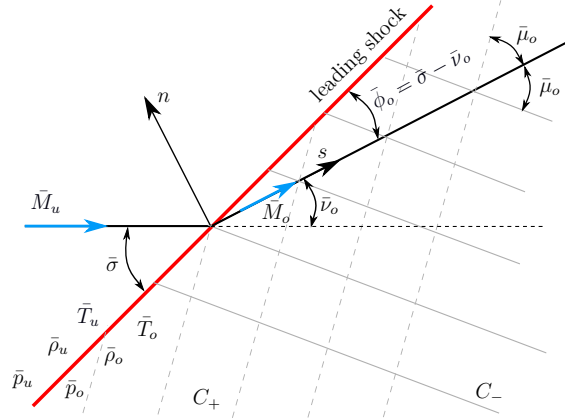


Fig. 2 Schematic view of the coordinate system and characteristic lines of the flow.

For weakly exothermic detonations, all three families of characteristics are straight lines with fixed inclination angles. In the cartesian coordinate system employed here the streamlines correspond to the lines $n = \text{constant}$, while the Mach lines are given by

$$C_{\pm} : \quad s - \frac{n}{\tan \bar{\phi}_o} = \left(\frac{-1}{\tan \bar{\phi}_o} \pm \frac{1}{\tan \bar{\mu}_o} \right) (n - n_s), \quad (14)$$

involving the inclination angle

$$\bar{\mu}_o = \sin^{-1} \left(\frac{1}{\bar{M}_o} \right) \quad (15)$$

and the value n_s of the coordinate n at which the Mach line intersects the shock, whose location is defined in this linear approximation by the straight line $s = n/\tan \bar{\phi}_o$. The condition that the normal component of the velocity behind the shock is subsonic, given in Eq. (A.11), implies that $\bar{\mu}_o > \bar{\phi}_o$, so that the C_+ characteristics always reach the shock, while the C_- characteristics originate there.

The problem can be conveniently expressed in characteristic form by combining linearly Eqs. (6), (7) and (11) to give

$$\frac{\partial I^+}{\partial s} + \frac{1}{\sqrt{\bar{M}_o^2 - 1}} \frac{\partial I^+}{\partial n} = \frac{\gamma \bar{M}_o^2}{\bar{M}_o^2 - 1} \Omega \quad (16)$$

and

$$\frac{\partial I^-}{\partial s} - \frac{1}{\sqrt{\bar{M}_o^2 - 1}} \frac{\partial I^-}{\partial n} = \frac{\gamma \bar{M}_o^2}{\bar{M}_o^2 - 1} \Omega \quad (17)$$

for the Riemann characteristic variables

$$I^\pm = \hat{p} \pm \frac{\gamma \bar{M}_o^2}{\sqrt{\bar{M}_o^2 - 1}} \hat{v}. \quad (18)$$

Using $\hat{p} = (I^+ + I^-)/2$ in (7) provides

$$\frac{\partial \hat{T}}{\partial s} - \frac{\gamma - 1}{2\gamma} \frac{\partial}{\partial s} (I^+ + I^-) = \Omega, \quad (19)$$

which, together with Eqs. (16), (17), and the conservation equations for chemical species are the basis for the description of the supersonic post-shock flow in two-dimensional, steady, weakly exothermic oblique detonations.

The integration of Eq. (19) along the streamlines and of Eq. (17) along the C_- characteristics is initiated at the shock $s = n/\tan \bar{\phi}_o$, where the values of \hat{T} and I^- depend on the value of I^+ reaching the shock from below. The derivation of the needed post-shock expressions for \hat{T} and I^- begins by using the definition (18) along with the linearized Rankine-Hugoniot relations given in Eq. (12) to relate the values of the characteristic variables I^\pm at the shock with the perturbations of upstream Mach number and incident angle according to

$$I^+ = A^+ \hat{M}_u + B^+ \hat{\sigma} \quad \text{and} \quad I^- = A^- \hat{M}_u + B^- \hat{\sigma} \quad (20)$$

where

$$A^\pm = A_p \pm \frac{\gamma M_o^2}{\sqrt{M_o^2 - 1}} A_v \quad \text{and} \quad B^\pm = B_p \pm \frac{\gamma M_o^2}{\sqrt{M_o^2 - 1}} B_v. \quad (21)$$

The first equation in (20) can be used to provide

$$\hat{\sigma} = -\frac{A^+}{B^+} \hat{M}_u + \frac{1}{B^+} I^+ \quad (22)$$

for the local incident angle as a function of the value of I^+ reaching the shock from below. Using this last equation in (12) and (20) finally yields the needed expressions

$$\hat{T} = \hat{T}_u + \left(A_T - \frac{B_T}{B^+} A^+ \right) \hat{M}_u + \frac{B_T}{B^+} I^+ \quad (23)$$

and

$$I^- = \left(A^- - \frac{B^-}{B^+} A^+ \right) \hat{M}_u + \frac{B^-}{B^+} I^+ \quad (24)$$

relating the post-shock values of \hat{T} and I^- with I^+ . The C_+ characteristics originate behind the shock and the initial conditions for integration of Eq. (16) depend on the specific problem considered. For example, if the post-shock flow is bounded by a straight wall, as in problems involving initiation of a detonation at a wedge [2], the initial value of I^+ at a given wall location is the value of I^- corresponding to the C^- characteristic reaching the wall at that location, as follows from the condition of zero normal velocity $\hat{V} = 0$.

III. One-Step Arrhenius Description

As previously mentioned, since the heat-release rate Ω depends in general on the mixture composition, Eqs. (16), (17), and (19) must be supplemented with Eq. (10), needed to compute the evolution of the species mass fractions along the streamlines. The number of chemical species and the accompanying expressions for the consumption rates ω_i depend on the specific reactant mixture considered. While the formulation is compatible with the use of detailed chemical-kinetic mechanisms with multiple chemical intermediates, a simple model consisting of an irreversible Arrhenius reaction that releases an amount of heat Q' per unit mass of reactant burnt suffices in many cases to describe the important nonlinear effects associated with the strong temperature sensitivity of the chemical reaction. It is assumed that the upstream mass fraction of reactant in the base solution \bar{Y}_u is such that the amount of heat released per unit of mass of gas mixture $Q = Q' \bar{Y}_u$ satisfies the condition $Q \ll c_p \bar{T}_o$, consistent with the approximation stated in Eq. (3). The mass of reactant consumed per unit volume per unit time will be described with the Arrhenius expression

$$\omega = \rho B Y \exp \left(-\frac{E_a}{R^o T} \right), \quad (25)$$

in terms of the density ρ , temperature T , and reactant mass fraction Y . Here B is a preexponential factor, R^o is the universal gas constant, and E_a is the activation energy. The following description considers large values of the dimensionless activation energy

$$\frac{E_a}{R^o \bar{T}_o} \sim \left(\frac{Q}{c_p \bar{T}_o} \right)^{-1} \gg 1, \quad (26)$$

for which relative temperature variations of order $q = Q/(c_p \bar{T}_o)$ across the reaction layer result in reaction-rate changes of order unity. In writing the temperature dependence of the reaction rate use is made of the familiar Frank-Kamenetskii linearization

$$\exp\left(-\frac{E_a}{R^\circ T}\right) \simeq \exp\left(-\frac{E_a}{R^\circ \bar{T}_o}\right) \exp\left(\beta \frac{(T - \bar{T}_o)/\bar{T}_o}{q}\right), \quad (27)$$

involving the reduced activation energy

$$\beta = \left(\frac{E_a}{R^\circ \bar{T}_o}\right) \left(\frac{Q}{c_p \bar{T}_o}\right), \quad (28)$$

an order-unity parameter in the distinguished limit defined in Eq. (26). The reaction-rate defined in (25) leads to the selection

$$t_i = B^{-1} \exp\left(\frac{E_a}{R^\circ \bar{T}_o}\right) \quad (29)$$

for the characteristic induction time used in scaling s and n , reducing the heat-release rate to

$$\Omega = y e^{\beta \hat{T}} \quad (30)$$

and the reactant conservation equation (10) to

$$\frac{\partial y}{\partial s} = -\Omega = -y e^{\beta \hat{T}}, \quad (31)$$

where $y = Y/\bar{Y}_u$. The boundary condition for the reactant mass fraction behind the chemically frozen shock reduces to $y = y_u$, where $y_u = Y_u/\bar{Y}_u$ differs from unity when the composition of the incoming stream is nonuniform.

The one-step-chemistry problem can be readily solved for an unperturbed detonation with $\sigma = \bar{\sigma}$, whose inner structure depends only on the distance $x = s \sin \bar{\phi}_o - n \cos \bar{\phi}_o$ to the shock. Straightforward integration of (6), (7), (11) and (31) subject to the conditions $\hat{T} = \hat{p} = \hat{V} = y - 1 = 0$ at $x = 0$ yields

$$1 - y = \frac{1 - \bar{M}_o^2 \sin^2 \bar{\phi}_o}{1 - \gamma \bar{M}_o^2 \sin^2 \bar{\phi}_o} \hat{T} = -\frac{1 - \bar{M}_o^2 \sin^2 \bar{\phi}_o}{\gamma \bar{M}_o^2 \sin^2 \bar{\phi}_o} \hat{p} = -\frac{1 - \bar{M}_o^2 \sin^2 \bar{\phi}_o}{\sin \bar{\phi}_o \cos \bar{\phi}_o} \hat{V} \quad (32)$$

and

$$x/\sin \bar{\phi}_o = s - n/\tan \bar{\phi}_o = e^{-\beta Z} [E_i(\beta Z) - E_i(\beta Z y)], \quad (33)$$

where E_i is the exponential integral function and

$$\beta Z = \frac{E_a}{R^\circ \bar{T}_o} \frac{T_b - \bar{T}_o}{\bar{T}_o} = \frac{1 - \gamma \bar{M}_o^2 \sin^2 \bar{\phi}_o}{1 - \bar{M}_o^2 \sin^2 \bar{\phi}_o} \beta \quad (34)$$

is the Zeldovich number of the base flow. Equation (33) describes the decay of the reactant mass fraction with the

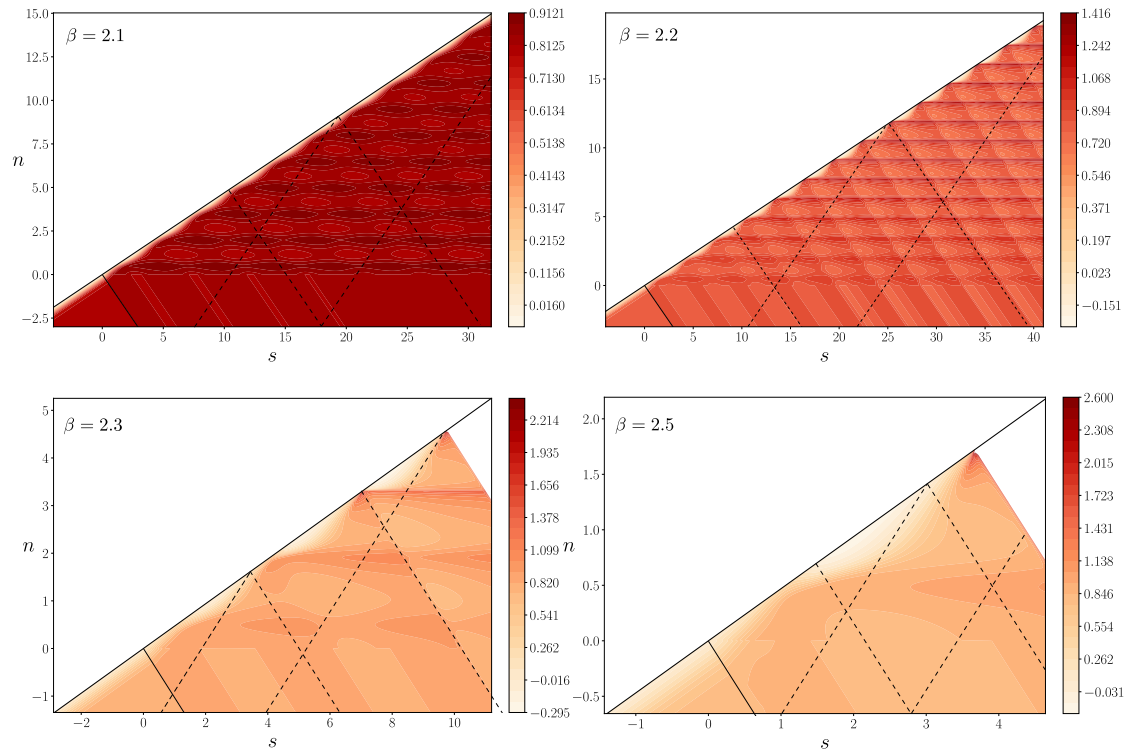


Fig. 4 Temperature distributions behind the shock for a detonation with $\bar{M}_u = 2.5$ and $\sigma = 50^\circ$ interacting with a vortex sheet with $\hat{M}_u = 1$.

initial value $\hat{\sigma} = -(A^+/B^+)\hat{M}_u$, as follows from Eq. (22) with $I^+ = 0$. The incident angle is seen to oscillate about this value following the sequential pressure-wave reflections between the reaction layer and the leading shock.

For $\beta = 2.1$ (and also for smaller values of β) these oscillations decay, and the detonation structure approaches a one-dimensional solution with an induction length that is smaller than that of the original solution because of the higher post-shock temperature associated with the Mach-number increment. By way of contrast, for values of the activation energy larger than $\beta \simeq 2.15$ the oscillation amplitude increases. For $\beta = 2.2$ the reinforcement of the shock strength by the coupling of the pressure oscillations with the chemical reaction reaches saturation, and the solution develops a nonlinear, spatially periodic structure that prevails indefinitely downstream. These oscillatory structures are reminiscent of the cellular structures observed in wedge-induced configurations [6, 8]. The results for $\beta = 2.3$ and $\beta = 2.4$ show that a further increase in β results in the development of a local explosion at a localized position along the leading shock after a finite number of oscillations, marking the formation of a triple point. The divergence that is observed marks the failure of the Frank-Kamenetskii linearization, which remains fundamentally inapplicable subsequent to the initial divergence, requiring the full Arrhenius rate expression to be employed for accurate predictions after that, even though the strength of the triple point is limited by the small parameter q . The formulation, exclusive of the (internally consistent) chemical-kinetic approximation, thus remains applicable, but it would require a revised description of the

heat-release rate to address the post-explosion evolution.

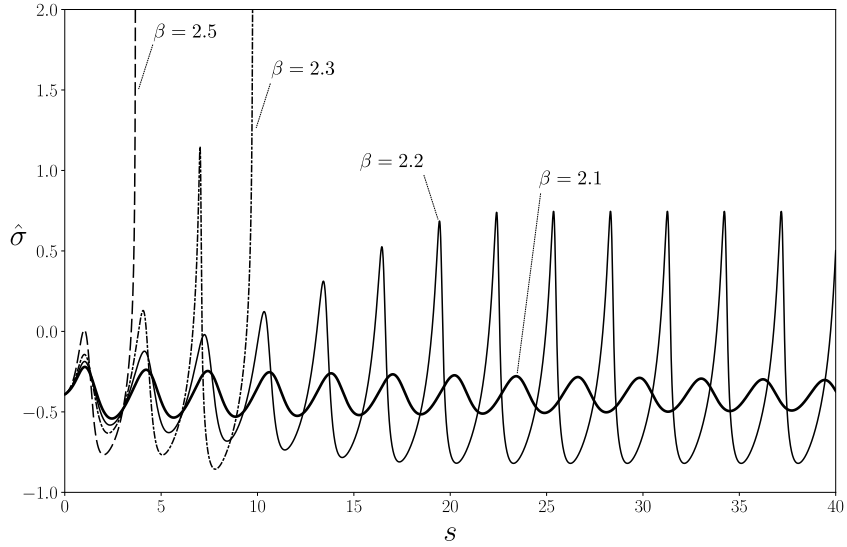


Fig. 5 Spatial variation of the incidence angle $\hat{\sigma}$ for the detonations of Fig. 4.

V. Conclusions

It may be concluded from these observations that the wide range of oblique-detonation phenomena, including spatial oscillations and abrupt transitions, that have been discovered through full numerical simulations, are present even when the heat release is small compared with the post-shock thermal enthalpy. For conditions under which that limit of small q is reasonable, the much simpler formulation derived herein significantly reduces the complexity of the computations and decreases the number of parameters involved, making thorough parametric investigations more accessible. The reduced complexity also facilitates improvement of physical understanding of the results. The approach, moreover, is not limited to any particular class of chemical-kinetic descriptions but instead can handle arbitrary descriptions of heat-release rates. For these reasons, it would be of interest to exploit this formulation further by considering more elaborate chemical kinetics and additional configurations, such as oblique-detonation impingement on distributed mixing layers and oblique detonations anchored by wedges.

Appendix - Jump Conditions and Their Linearization

As shown by Gross [14], in the constant-specific-heat approximation the relationships between the initial values and the final equilibrium values of parameters for oblique detonations can be conveniently written in terms of the density

ratio

$$\frac{\rho_u}{\rho_b} = R = 1 - \frac{M_u^2 \sin^2 \sigma - 1}{(\gamma + 1)M_u^2 \sin^2 \sigma} \left[1 + \left(1 - \frac{2(\gamma + 1)M_u^2 \sin^2 \sigma}{(M_u^2 \sin^2 \sigma - 1)^2} \frac{Q}{c_p T_u} \right)^{1/2} \right] \quad (\text{A.1})$$

according to

$$\frac{p_b}{p_u} = 1 + \gamma M_u^2 \sin^2 \sigma (1 - R), \quad (\text{A.2})$$

$$\frac{T_b}{T_u} = R [1 + \gamma M_u^2 \sin^2 \sigma (1 - R)], \quad (\text{A.3})$$

$$M_b = M_u \left[\frac{1 - \sin^2 \sigma (1 - R^2)}{R [1 + \gamma M_u^2 \sin^2 \sigma (1 - R)]} \right]^{1/2}, \quad (\text{A.4})$$

and

$$\nu_b = \sigma - \cos^{-1} \left[\frac{\cos \sigma}{[1 - \sin^2 \sigma (1 - R^2)]^{1/2}} \right], \quad (\text{A.5})$$

where γ is the specific-heat ratio, Q is the heat released per unit mass of gas mixture, and c_p is the specific heat at constant pressure. The conditions immediately behind the shock can be computed simply by setting $Q = 0$ in the above expressions, leading to the well-known equations

$$\frac{\rho_o}{\rho_u} = F_\rho(M_u, \sigma) = \frac{(\gamma + 1)M_u^2 \sin^2 \sigma}{(\gamma - 1)M_u^2 \sin^2 \sigma + 2} \quad (\text{A.6})$$

$$\frac{p_o}{p_u} = F_p(M_u, \sigma) = \frac{2\gamma M_u^2 \sin^2 \sigma + 1 - \gamma}{\gamma + 1}, \quad (\text{A.7})$$

$$\frac{T_o}{T_u} = F_T(M_u, \sigma) = \frac{[2\gamma M_u^2 \sin^2 \sigma + 1 - \gamma][(\gamma - 1)M_u^2 \sin^2 \sigma + 2]}{(\gamma + 1)^2 M_u^2 \sin^2 \sigma} \quad (\text{A.8})$$

$$M_o = F_M(M_u, \sigma) = \frac{1}{\sin \phi_o} \left[\frac{2 + (\gamma - 1)M_u^2 \sin^2 \sigma}{2\gamma M_u^2 \sin^2 \sigma + 1 - \gamma} \right]^{1/2}, \quad (\text{A.9})$$

$$\nu_o = F_\nu(M_u, \sigma) = \tan^{-1} \left\{ \frac{2(M_u^2 \sin^2 \sigma - 1) \cot \sigma}{2 + M_u^2 [\gamma + \cos(2\sigma)]} \right\}, \quad (\text{A.10})$$

where the angle

$$\phi_o = \sigma - \nu_o$$

appearing in Eq. (A.9) measures the inclination of the post-shock stream with respect to the shock. The post-shock velocity normal to the shock is subsonic, so that the associated Mach number satisfies

$$M_{o_n} = M_o \sin \phi_o < 1. \quad (\text{A.11})$$

Values of M_o and M_{o_n} are plotted on the $\sigma - M_u$ plane of Fig. 6 for $\gamma = 1.4$. The top and bottom thick solid curves on the plot indicate conditions under which the post-shock flow is sonic (i.e. $M_o = 1$) and the shock is infinitesimally weak (i.e. $M_u \sin \sigma = 1$), the latter coinciding with the iso-curve $M_{o_n} = 1$.

For weakly exothermic detonations with small heat release the relative variations of all flow properties across the reaction region and the associated deflection of the streamlines are small, of order $Q/(c_p T_o) \ll 1$, as can be seen by linearizing Eqs. (A.1)–(A.5) for small Q to give

$$-\frac{\rho_b - \rho_o}{\rho_o} = -\frac{(p_b - p_o)/p_o}{\gamma M_o^2 \sin^2 \phi_o} = \frac{(T_b - T_o)/T_o}{1 - \gamma M_o^2 \sin^2 \phi_o} = \frac{v_o - v_b}{\cos \phi_o \sin \phi_o} = \frac{Q/(c_p T_o)}{1 - M_o^2 \sin^2 \phi_o}. \quad (\text{A.12})$$

The expression for the temperature change indicates that for detonations with $\gamma M_o^2 \sin^2 \phi_o = 1$ (i.e. $M_{o_n} = \gamma^{-1/2}$) the rate of heat release behind the shock balances exactly the compression work, in such a way that the resulting equilibrium temperature remains equal to the post-shock temperature. These thermally neutral conditions are indicated on the $\sigma - M_u$ diagram of Fig. 6. As can be seen from the plot, there exists a small parametric region bounded by the curves $M_u \sin \sigma = 1$ and $\gamma M_o^2 \sin^2 \phi_o = 1$, corresponding to very weak leading shocks, where the temperature decreases downstream from the shock as the exothermic chemical reaction takes place. Most cases of interest lie above the curve $\gamma M_o^2 \sin^2 \phi_o = 1$, for which the temperature increases as the pressure decreases behind the shock.

In the present formulation, the jump conditions across the shock for the perturbations of pressure, temperature, and transverse velocity are given by the linearized form of the Rankine-Hugoniot relations, given in Eq. (12). The coefficients involved in the linearized expressions, defined in Eq. (13), can be computed by differentiating Eqs. (A.7), (A.8), and (A.10) to give

$$\left. \begin{aligned} M_u A_T = \tan \sigma B_T &= \frac{4(\gamma - 1)(\gamma M_u^4 \sin^4 \sigma + 1)}{[2\gamma M_u^2 \sin^2 \sigma + 1 - \gamma][(\gamma - 1)M_u^2 \sin^2 \sigma + 2]} \\ M_u A_p = \tan \sigma B_p &= \frac{4\gamma M_u^2 \sin^2 \sigma}{2\gamma M_u^2 \sin^2 \sigma + 1 - \gamma} \\ A_v &= \frac{4(\gamma + 1)M_u \cot \sigma}{(\gamma^2 + 1)M_u^4 + 2\gamma M_u^4 \cos(2\sigma) + 4(\gamma - 1)M_u^2 + 4 \csc^2(\sigma)} \\ B_v &= -2 \frac{M_u^2 [\gamma M_u^2 \cos(2\sigma) + M_u^2 - 4] + [(\gamma + 1)M_u^2 + 2] \csc^2(\sigma)}{(\gamma^2 + 1)M_u^4 + 2\gamma M_u^4 \cos(2\sigma) + 4(\gamma - 1)M_u^2 + 4 \csc^2(\sigma)} \end{aligned} \right\} \quad (\text{A.13})$$

Funding Sources

The work of DMR and CH was supported by the Spanish Ministry of Science through grant # ENE2015-65852-C2-1-R) and by the Fundación Iberdrola España through grant # BYNV-ua37crdy. The work of ALS and FAW was supported by the US AFOSR Grant No. FA9550-16-1-0443.

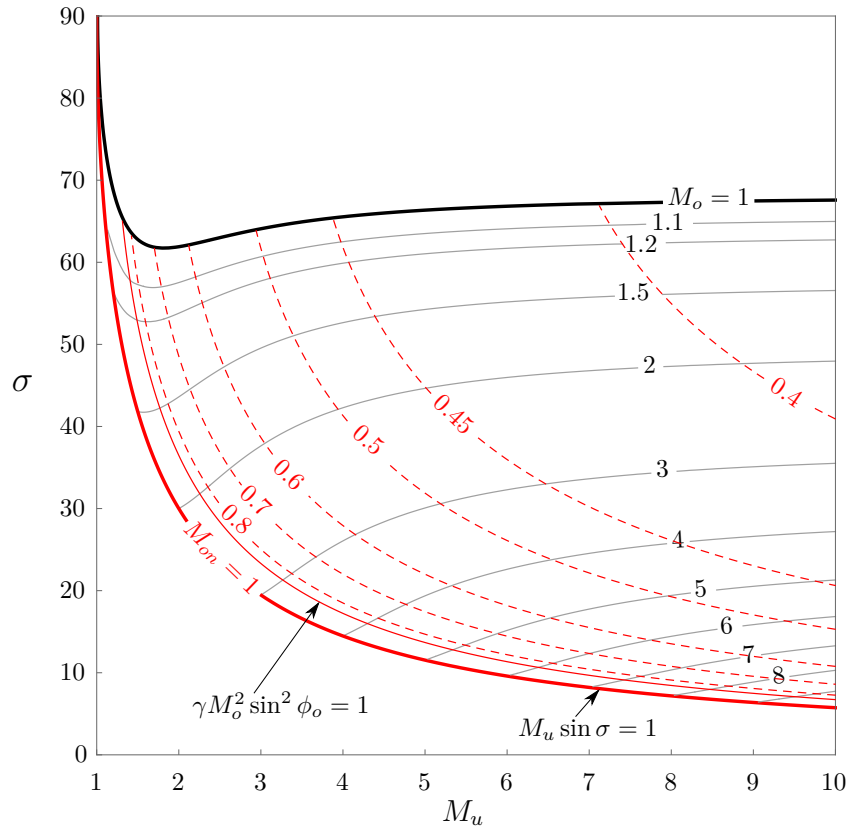


Fig. 6 Values of the post-shock Mach numbers M_o and $M_{on} = M_o \sin \phi_o$ behind an oblique shock for $\gamma = 1.4$.

References

- [1] Kailasanath, K., "Review of propulsion applications of detonation waves," *AIAA Journal*, Vol. 38, No. 9, 2000, pp. 1698–1708.
- [2] Li, C., Kailasanath, K., and Oran, E. S., "Detonation structures behind oblique shocks," *Physics of Fluids*, Vol. 6, No. 4, 1994, pp. 1600–1611.
- [3] Thaker, A., and Chelliah, H., "Numerical prediction of oblique detonation wave structures using detailed and reduced reaction mechanisms," *Combustion Theory and Modelling*, Vol. 1, No. 4, 1997, pp. 347–376.
- [4] Papalexandris, M. V., "A numerical study of wedge-induced detonations," *Combustion and Flame*, Vol. 120, No. 4, 2000, pp. 526–538.
- [5] Da Silva, L. F. F., and Deshaies, B., "Stabilization of an oblique detonation wave by a wedge: a parametric numerical study," *Combustion and Flame*, Vol. 121, No. 1-2, 2000, pp. 152–166.
- [6] Choi, J.-Y., Kim, D.-W., Jeung, I.-S., Ma, F., and Yang, V., "Cell-like structure of unstable oblique detonation wave from high-resolution numerical simulation," *Proceedings of the Combustion Institute*, Vol. 31, No. 2, 2007, pp. 2473–2480.
- [7] Teng, H. H., and Jiang, Z. L., "On the transition pattern of the oblique detonation structure," *Journal of Fluid Mechanics*, Vol. 713, 2012, pp. 659–669.

- [8] Verreault, J., Higgins, A. J., and Stowe, R. A., "Formation of transverse waves in oblique detonations," *Proceedings of the Combustion Institute*, Vol. 34, No. 2, 2013, pp. 1913–1920.
- [9] Powers, J. M., and Stewart, D. S., "Approximate solutions for oblique detonations in the hypersonic limit," *AIAA Journal*, Vol. 30, No. 3, 1992, pp. 726–736.
- [10] Huete, C., Sánchez, A. L., Williams, F. A., and Urzay, J., "Diffusion-flame ignition by shock-wave impingement on a supersonic mixing layer," *Journal of Fluid Mechanics*, Vol. 784, 2015, pp. 74–108.
- [11] Huete, C., Sánchez, A. L., and Williams, F. A., "Diffusion-flame ignition by shock-wave impingement on a hydrogen–air supersonic mixing layer," *Journal of Propulsion and Power*, 2016, pp. 256–263.
- [12] Clavin, P., and Williams, F. A., "Analytical studies of the dynamics of gaseous detonations," *Philos. Trans. A Math. Phys. Eng. Sci.*, Vol. 370, No. 1960, 2012, pp. 597–624.
- [13] Williams, F. A., *Combustion theory*, Cummings Publ. Co, 1985.
- [14] Gross, R., "Oblique detonation waves," *AIAA Journal*, Vol. 1, No. 5, 1963, pp. 1225–1227.
- [15] Huete, C., Sánchez, A. L., and Williams, F. A., "Linear theory for the interaction of small-scale turbulence with overdriven detonations," *Physics of Fluids*, Vol. 26, No. 11, 2014, p. 116101.
- [16] Hayes, W. D., Probstein, R. F., and Probstein, R. R., *Hypersonic inviscid flow*, Courier Corporation, 2004.